# Cell Flow PET Simulations for Validation of Cell Tracking Algorithms

N. Marquardt[1], T. Hengsbach[1], M. Mauritz[2], B. Wirth[2], K. P. Schäfers[1]

[1]European Institute for Molecular Imaging, University of Münster, Germany; [2]Institute for Computational and Applied Mathematics, University of Münster, Germany

Contact: n.marquardt@uni-muenster.de

## Introduction

Recently, new reconstruction algorithms for positron emission tomography (PET) using optimal transport-based regularization have been developed to dynamically track single or multiple radioactively labeled cells in a simulated human body [1, 2] . To further enhance and validate these algorithms, we are creating simulations that realistically model cell flow in clinical scenarios and generate raw PET data through Monte Carlo simulations. The cells' locations and movements are tracked continuously as ground-truth data. The described cell flow PET simulation (CeFloPS) is based on the XCAT phantom [3] (Fig. 1) and extends our earlier work [4].

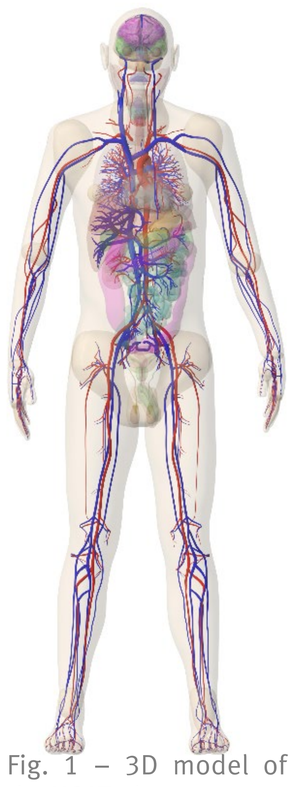

Fig. 1 – 3D model of the XCAT phantom.

## Methods

The cell path simulation in CeFloPS can be divided into a blood flow part and an organ distribution part, followed by the Monte-Carlo PET simulation using GATE [5].

Blood flow simulation

- Simplification of XCAT blood vessel system to 1mm-spaced node structure (Fig. 2)
- Calculation of blood flow $Q$ in each node using Kirchhoff's laws and Hagen-Poiseuille equation:

$$Q = {\Delta P}/{R}, \qquad R = {8l\eta}/{\pi r^4}$$

- Probabilistic decision of cell path at bifurcations using blood flow distribution
- Assuming laminar flow, the cell velocity profile is given by

$$v(x) = {2\bar{Q}}/{\pi r^2}\left(1 - {x^2}/{r^2}\right)$$

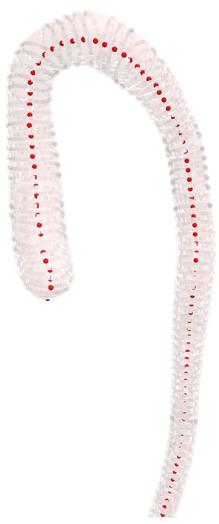

Fig. 2 – Node structure in the aorta.

Organ distribution simulation

- Organs are voxelized with voxel size $(0.5\text{mm})^3$
- Voxels with artery entry or vein exit are identified
- Probability vector field for cell motion in organ is calculated with arteries/veins as sources/sinks (Fig. 3)
- Cells perform 3D random walk biased with the probability vectors from artery entry to vein exit
- Duration of random walk is determined by physiologically based modelling

**For animated versions of the results, scan the code to the left!**

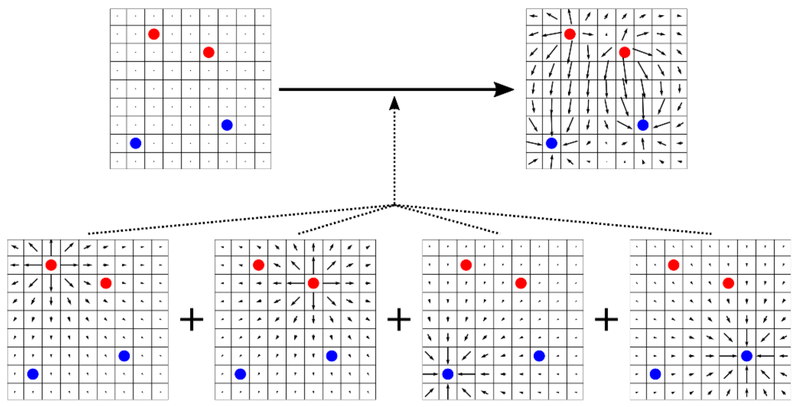

Fig. 3 – 2D representation of the probability vector field used for the random walk inside an organ (red: artery entries, blue: vein exits).

- Inside an organ, a cell can be located in different compartments (number and form depending on cell of interest, Fig. 4)
- Transition between compartments are governed by transition matrix $G$ with rate constants $k_i$,
- Probability $\Pi$ of cell movement to next voxel is determined using the transition matrix and the length of a time step $\Delta t$:

$$\Pi = \exp(\Delta t G)$$

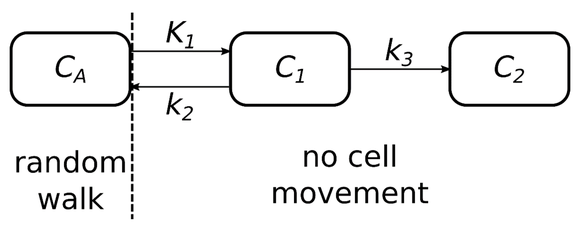


Fig. 4 – Compartment model structure and rate constants for cells behaving like FDG tracer in an organ. Only cells located in $C_A$ undergo random walk, cells in $C_2$ are trapped for the rest of the simulation.

Monte-Carlo PET simulation

- Spatial coordinates of cells as input for moving radioactive sources in GATE
- Total-body scanner Siemens Biograph Vision Quadra (Siemens Healthineers) implemented as base for simulations
- XCAT phantom for attenuation and scatter effects
- Lutetium-176 background from LSO crystals can be simulated

## Results

As an example, the movement of 10 cells with transition rates from [6] and 10kBq each were simulated for 600s in 10ms steps using CeFloPS and GATE (without background). To account for different activities, the resulting PET data was cut to only account for 20%, 5% and 1% of the simulated coincidences. The resulting data was reconstructed using a new algorithm based on optimal transport (dyn opt)[2] and a classical frame-wise expectation maximization method (fw EM). To compare both, the time window from 109s to 120s was selected and split into 23 frames (Fig. 5, 6). The difference to the ground truth for both methods was calculated using the metric described in [7] (Tab. 1).

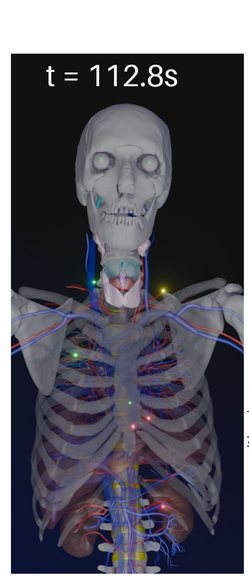


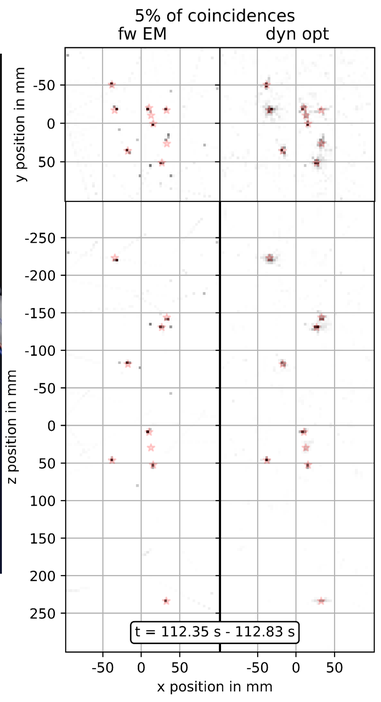


Fig. 5 – Left: Locations of 10 simulated cells in XCAT phantom (red: cells in $C_A$, yellow: $C_1$, green: $C_2$). Right: reconstructed positions using fw EM and dyn opt (red stars: ground truth positions).

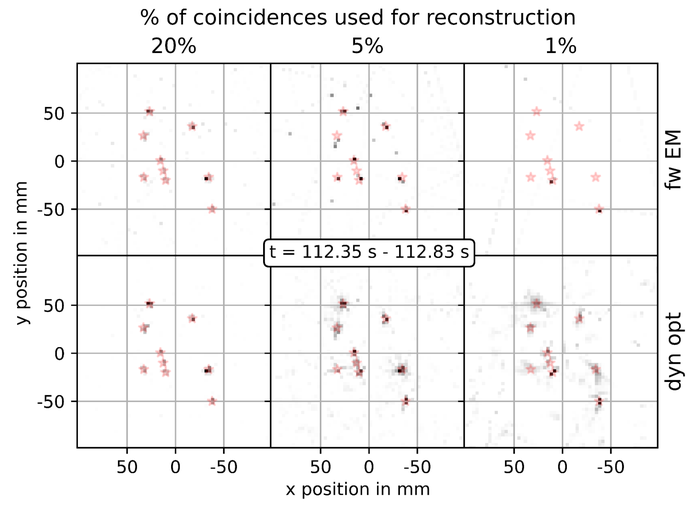


Fig. 6 – Reconstructions for different numbers of coincidences used.

Tab. 1 – Positional error of fw EM and dyn opt compared to ground truth for different numbers of used coincidences and maximal regarded transport distances of cells as defined in [7] (1 px diameter = 5.8mm).

| % of coincidences used | Maximum transport in px diameter | Positional error in mm | |
|---|---|---|---|
| | | fw EM | dyn opt |
| 20 | 2 | 7.9 | 6.6 |
| | 5 | 18.7 | 15.5 |
| | 10 | 35.3 | 30.4 |
| 5 | 2 | 8.7 | 8.0 |
| | 5 | 20.2 | 17.1 |
| | 10 | 38.0 | 32.0 |
| 1 | 2 | 10.3 | 9.0 |
| | 5 | 24.8 | 18.7 |
| | 10 | 46.7 | 33.6 |

## Conclusion

CeFloPS offers a promising approach to simulate realistic cell paths in the human body which mimic clinical situations. The PET data generated with CeFloPS and GATE, together with the knowledge of the ground-truth positions of the cells, allow to quantitatively validate and improve new reconstruction algorithms which are able to track single or multiple cells with PET.

## References

[1] Schmitzer, B., Schäfers, K.P., Wirth, B. (2019), IEEE Transactions on Medical Imaging 39: 1626-1635.
[2] Mauritz, M., Schmitzer, B., Wirth, B. (2024), SIAM Journal on Mathematical Analysis, 56(5), 5840-5880.
[3] Segars, W.P., Sturgeon, G., Mendonca, S., Grimes, J., Tsui, B.M.W. (2010). Med. Phys., 37: 4902-4915.
[4] Marquardt, N., Schäfers, K.P. (2023), 2023 IEEE NSS MIC RTSD.
[5] Jan, S., Santin, G., Strul, D., et al. (2004). Phys Med Biol., 49(19): 4543-4561.
[6] Li, E.J., Spencer, B.A., Schmall, J.P., Abdelhafez, Y., Badawi, R.D., Wang, G., Cherry, S.R. (2022). Journal of Nuclear Medicine, 63(8), 1266-1273.
[7] Chizat, L., Peyré, G., Schmitzer, B. et al. (2018) Found Comput Math 18, 1–44.

Funded by DFG Deutsche Forschungsgemeinschaft German Research Foundation

inSight CRC 1450

This work was funded by the Deutsche Forschungsgemeinschaft (DFG) – CRC 1450 – 431460824